

## On the structure of organic-coated water droplets: From “net water attractors” to “oily” drops

Purnendu Chakraborty<sup>1</sup> and Michael R. Zachariah<sup>1,2</sup>

Received 16 March 2011; revised 16 August 2011; accepted 18 August 2011; published 12 November 2011.

[1] Organic-coated aerosols are believed to play an important role in atmospheric processes thereby influencing global climate. In our earlier works involving water droplets coated with hydrocarbon chains (<sup>12</sup>C, dodecanoic acid) we found that these particles prefer an inverted micelle structure with an aqueous core and a hydrophobic surface. Such particles maintained their overall spherical shapes (with a spherical water-fatty acid interface) leading to a negative surface tension. Consequently, such particles were seen to be net “water attractors” despite a hydrophobic surface. In this paper, we report the results of molecular dynamics studies, in which we investigated the effect of fatty acid chain length, chain branching, and terminal group on the morphology and properties of water droplets coated with organics. It has been seen that for particles coated with longer/branched surfactants, the fatty acid chains tend to align parallel to each other, forcing local flattening and significant distortion of the underlying water substrate. Sticking coefficient calculations of water vapor on such particles showed that these newly formed particles behave in a manner that is consistent with an “oily” surface as opposed to particles with shorter chains that can process water and are “net water attractors.”

**Citation:** Chakraborty, P., and M. R. Zachariah (2011), On the structure of organic-coated water droplets: From “net water attractors” to “oily” drops, *J. Geophys. Res.*, 116, D21205, doi:10.1029/2011JD015961.

### 1. Introduction

[2] Aerosol particles play a major role in global climate and perhaps climate change. A significant part of this effect is by acting as cloud condensation nuclei (CCN) and hence moderating the radiative properties of clouds.

[3] It is believed that as marine aerosol particles form, they acquire a coating of organic origin [Blanchard, 1964; Ellison *et al.*, 1999; Gill *et al.*, 1983; Middlebrook *et al.*, 1998]. There had only been indirect evidence [Baier, 1972; Blanchard, 1964; Ellison *et al.*, 1999; Gill *et al.*, 1983; Husar and Shu, 1975; MacIntyre, 1972, 1974; Middlebrook *et al.*, 1998] to support this theory based on the fact that amphiphilic molecules can self-assemble as monolayers at air-water interfaces [Blodgett, 1935; Langmuir, 1917]. In a more recent work, Tervahattu *et al.* [2002] found, using time-of-flight secondary mass spectrometry (TOF-SIMS), palmitic (hexadecanoic) acid distribution on small particles, similar to marine particles. Their results showed that fatty acids are important ingredients on the surface of marine aerosols. In a subsequent work [Tervahattu *et al.*, 2005], the existence of fatty acid population on a variety of continental aerosols was reported. By using TOF-SIMS, fatty acids of carbon chain lengths up to <sup>32</sup>C acids were found on sulfate aerosols.

[4] Ellison *et al.* [1999] proposed an “inverted micelle” structure for such organic aerosols, consisting of an aqueous core encapsulated in an inert hydrophobic organic monolayer. In the proposed model, the surfactants lie with their polar heads inserted into the ionic aqueous core and the hydrophobic hydrocarbon tails radially outward, exposed to the atmosphere. More recently, experimental evidence of surface segregation of organic/water systems has been provided in work by Wyslouzil *et al.* [2006]. Li and Wilemski [2006] were able to map the stability regions of binary water/organic droplets using Monte Carlo analysis.

[5] In our recent work [Chakraborty and Zachariah, 2007, 2008], using Coarse-Grained Molecular Dynamics (CGMD) [Lopez *et al.*, 2002; Shelley *et al.*, 2001a; Shelley *et al.*, 2001b] simulation, we observed that fatty acid coated water droplets indeed favored an inverted micelle-like structure as mentioned in the previous paragraph. The resulting profile of the normal component of the pressure tensor [Chakraborty and Zachariah, 2007, Figure 3] indicated that for such structures the coating would be under negative pressure, i.e., tension. Using a simple ball-stick model and force balance arguments, we showed that this negative pressure was a consequence of the curved (spherical) water-surfactant interface, which resulted in a larger separation between the hydrocarbon chains of the surfactants (and hence lower chain-chain interaction) with increasing radial distance. The tension in the coating led to a “negative surface tension.” It was argued that this negative surface tension would lead to an inverse Kelvin vapor pressure effect resulting in increased water condensation. To

<sup>1</sup>Department of Mechanical Engineering, University of Maryland, College Park, Maryland, USA.

<sup>2</sup>National Institute of Standards and Technology, Gaithersburg, Maryland, USA.

support the argument, a simulation was carried out in which water vapor was placed in the simulation cavity along with the coated drop and the system was allowed to evolve. The vapor phase water was seen to be absorbed into the particle indicating the propensity of such particles to process water despite their apparent hydrophobicity. It was thus concluded that surfactant-coated water might be a very efficient substrate for water condensation.

[6] Following this work, we made an attempt to quantify water processing [Chakraborty and Zachariah, 2008] by computing the sticking coefficient of water vapor on such coated particles. The sticking (mass accommodation) coefficient or sticking probability,  $\alpha$ , describes the probability of a gas molecule being incorporated into the liquid [Vieceli *et al.*, 2004] as

$$\alpha = \frac{\text{number of molecules absorbed into liquid}}{\text{number of molecules impinging the liquid surface}}. \quad (1)$$

[7] It was found that the rate of water uptake (the sticking coefficient) was essentially a constant for incident speeds of water molecules around their most probable speed at the particle temperature, with one in six/seven collisions resulting in a stick, as opposed to 100% sticking for water molecules impinging on pure water droplets. We also found that the evaporation rate of water from the coated particle was greatly reduced, and in fact too small to compute. This implied that these apparently oily droplets are in fact “net water attractors” even though the sticking coefficient was a factor of 6 smaller. If such structures are produced in sufficient concentration in the atmosphere, they may be important contributors in the cloud condensation process.

[8] Uptake rate of atmospherically important compounds by aqueous solutions through short and long chain organic films has been studied experimentally. A monolayer of hexanoic acid has been shown to reduce the uptake of  $\text{N}_2\text{O}_5$  by seawater aerosols by a factor of three to four [Thornton and Abbatt, 2005]. By measuring the fraction of  $\text{N}_2\text{O}_5$  that is converted to  $\text{HNO}_3$ , it was seen [Park *et al.*, 2007] that 1-hexanol films (providing ~60% coverage) reduces the conversion from 0.15 to 0.06, whereas 1-butanol films (~44% coverage) reduces the conversion to 0.10. Monolayers of short chain organic amphiphiles have been seen to impede aqueous surface hydrolysis [Clifford *et al.*, 2007]. Whereas a  $^{18}\text{C}$  straight chain alcohol reduces the uptake of acetic acid by water, a branched version of the alcohol was found not to affect the uptake rate of acetic acid significantly [Gilman and Vaida, 2006]. Measurement of permeability of acetic acid through a mixed film of various chain lengths were found to be in between those through single-component films. [Gilman and Vaida, 2006]. In this work, we extend our studies to look at the effect of hydrocarbon chain length and chain branching on the structure and water-processing abilities of organic-coated aerosols. In addition, we briefly look at water droplets coated with dicarboxylic acids. The issue of solubility of shorter-chain dicarboxylic acids is taken up in a separate article [Ma *et al.*, 2011].

## 2. Computational Model and Simulation Details

[9] The molecular dynamics (MD) simulations in this work were performed using the software LAMMPS

[Plimpton, 1995] implemented on a parallel architecture. We used the tetrahedral SPC/E [Berendsen *et al.*, 1981, 1987] water model with an OH distance of 0.1 nm, point charges on the oxygen and hydrogen positions equal to  $-0.8476$  and  $+0.4328$  e (electronic charge unit), respectively, and a Lennard-Jones (LJ) interaction on the oxygen positions, given by

$$V(r) = 4\epsilon \left[ \left( \frac{\sigma}{r} \right)^{12} - \left( \frac{\sigma}{r} \right)^6 \right], \quad (2)$$

where  $r$  is the distance between two oxygen atoms. For these short-range force calculations the switched Lennard-Jones potential (regular LJ up to 1.0 nm, after which it is switched off to reach zero at a distance of 1.2 nm) was used. The SHAKE algorithm [Ryckaert *et al.*, 1977] was used to maintain the rigidity of the water molecules (fixed OH length and HOH angle).

[10] The surfactant molecules were modeled using both “united atom” setup (each hydrocarbon group was represented by a single site with interactions defined between these sites) and “fully atomistic” setup (to represent the carboxylic group). The bond stretchings and bond angle vibrations were represented by harmonic potentials. For the proper dihedral interaction, the periodic function  $V(\phi_{ijkl}) = k_\phi [1 + \cos(n\phi - \phi_0)]$  is chosen, where  $\phi$  is the angle between  $ijk$  and  $jkl$  planes and with zero corresponding to the *cis* configuration. The harmonic improper potential was used to keep a planar group planar. Finally, the O-H bond in the polar carboxylic group was kept rigid using the SHAKE algorithm. Both bonded and nonbonded potential parameters for all interactions were obtained from the GROMACS force field [Berendsen *et al.*, 1995; Lindahl *et al.*, 2001]. The equations of motion were integrated using the velocity form of the Verlet algorithm with a time step of 2 fs [Allen and Tildesley, 1987]. The simulations were conducted in vacuum, typically running on eight processors. During the equilibration, process temperature was controlled by rescaling velocities every few time steps. All other calculations were carried out in a constant energy environment.

[11] The first step was to create a pure water droplet. For this, a simple cubic structure was first generated with the oxygen atom at the vertex of each cube. Water molecules within a certain radius were considered, resulting in an initial spherical configuration consisting of 2440 water molecules. Generating velocities corresponding to 200 K, an equilibration simulation (at 200 K) was run for 50 ps. The water droplet was then slowly heated to 260 K over 120 ps resulting in an equilibrated water droplet. Next, the surface water molecules were identified and the fatty acid molecules were attached to these surface molecules with the polar head binding to the water substrate, and the hydrocarbon tail radially outward. After an energy minimization step, the particle was equilibrated at 260 K. Following that, the coated particle was heated to 300 K and allowed to equilibrate at that temperature.

[12] For the sticking coefficient calculations, 100 water molecules (water monomers) were randomly placed at a distance of 6–7 nm from the center of the particle (so that initially there was no interaction between the added water molecule and the particle) and given a velocity toward the center. Since the sticking coefficient of water vapor on a

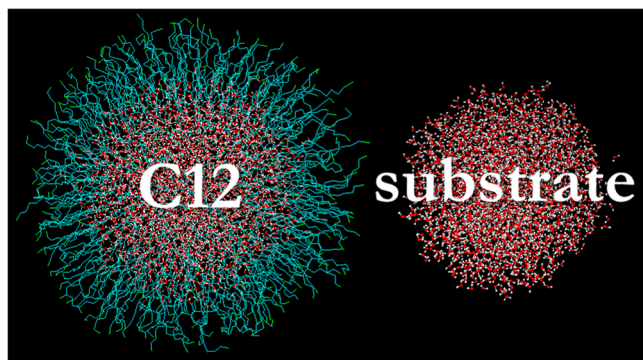


**Figure 1.** Equilibrated  $^{12}\text{C}$  particle ( $\sim 8$  nm in diameter with an organic coating  $\sim 2$  nm thick) along with the underlying substrate.

coated particle is essentially a constant [Chakraborty and Zachariah, 2008] around the most probable speed (corresponding to the particle temperature), the calculations in this work were carried out for the most probable speed. Except where noted, the angle of incidence of the impinging water monomer is zero degrees.

### 3. Water Droplet Coated With Organics: Structure and Water-Processing Abilities

[13] To study the effect of hydrocarbon chain length and branching, a total of four particles:  $^5\text{C}$ ,  $^{12}\text{C}$ ,  $^{28}\text{C}$ , and phytic acid (PHT), as explained below, were considered.

#### 3.1. Carbon-12-Coated and $^5\text{C}$ -Coated Droplets

[14] We begin with a  $^{12}\text{C}$ -coated water droplet (the “12” refers to the number of carbon atoms in the fatty acid molecule) consisting of 2440 water molecules and 505 dodecanoic acid molecules ( $\sim 8$  nm in diameter with a coating of  $\sim 2$  nm). This particle was studied in detail in our earlier work on water accommodation [Chakraborty and Zachariah, 2008]. Figure 1 shows a snapshot of the equilibrated  $^{12}\text{C}$  particle along with the underlying water substrate. The particle clearly exhibits an inverted micelle structure with the polar head of surfactant molecules binding to the polar water surface and the hydrophobic hydrocarbon chains oriented radially outward. For the density profile of the  $^{12}\text{C}$  particle, [see Chakraborty and Zachariah, 2008, Figure 3]. The fatty acid stays on the surface with absolutely no dissolution into the water core. As argued in work by Chakraborty and Zachariah [2007], such a density profile and curved water-surfactant interface would result in a negative surface tension, the effect of which is to reduce the equilibrium vapor pressure of the coated particle, enabling the organic-coated particle to process water despite its apparent hydrophobic surface. As discussed in section 1, this  $^{12}\text{C}$  particle is a net water attractor. Very similar results were obtained for a  $^5\text{C}$  particle. The equilibrated particle exhibits the same core-shell structure, only with shorter chains.

[15] Sticking coefficient calculations showed that 18% of the collisions led to a stick, with the incident water molecule penetrating through the organic coating and diffusing into

the water core. Like  $^{12}\text{C}$ ,  $^5\text{C}$  particles are also net water attractors.

[16] To study the effect of the angle of incidence on the sticking coefficient, three different angles of incidence of the impinging water monomer on the  $^5\text{C}$  particle were studied. For a given angle of incidence  $\theta$ , and an original monomer position (obtained for the normal incidence case), a new position was generated by rotating about an axis tangent to the particle surface at the point of intersection of the original position vector and the particle surface such that the velocity vector made an angle  $\pi - \theta$  with the original position vector. The speed was the same as that used for the normal incidence case, i.e., the most probable speed. The results of the sticking coefficient calculations are summarized in Table 1. The sticking coefficient was not seen to decrease with an increase in the incident angle. This behavior is not altogether unexpected. No appreciable reduction in the sticking coefficient has been seen for monomers hitting the coated particle at speeds considerably less than the most probable speed at normal incidence [Chakraborty and Zachariah, 2008, Figure 6]. This is probably due to the fact that monomers hitting the particle at an angle are inside the region of influence of the particle for a longer period of time.

[17] The organic-coated particles considered in this work, are secondary aerosols, sometimes formed as a result of sea sprays, where the surfactants coating the surface of the ocean originate from the decomposition of marine organisms, e.g., phytoplankton. It is quite possible that subsequent to the initial droplet formation the particles that do not get fully coated can either evaporate water from the exposed water surface or could process additional organic material from the atmosphere. To study the latter possibility, we placed a single surfactant molecule at 6 nm from the center of the particle and directed it toward the particle with its most probable speed at the given temperature. To obtain reasonable statistics, 100 such cases were considered, and it was found that all such collisions resulted in the impinging surfactant molecule sticking to the surface of the particle. Figure 2 shows snapshots of a typical collision simulation. After hitting the surface of the particle, the fatty acid molecule penetrates the coating and goes through a process of rearrangement till its polar head finally tethers to the polar water surface. It should be noted here that that the  $^{12}\text{C}$  particle was not likely to be 100% coated to begin with. Thus, our simulations show that partially coated organic aerosols can acquire a greater organic coverage through atmospheric surfactant molecules attaching to the surface.

#### 3.2. Carbon-28-Coated Droplets

[18] To assess the role of chain length, a sixteen-hydrocarbon chain was added to each of the surfactant molecules of the  $^{12}\text{C}$  particle to form the  $^{28}\text{C}$  particle. Figure 3 shows a

**Table 1.** Sticking Coefficient of Water Monomers at Different Angles of Incidence on the  $^5\text{C}$  Particle

Angle of Incidence	Sticking Coefficient
$0^\circ$	0.18
$15^\circ$	0.16
$30^\circ$	0.15
$60^\circ$	0.21

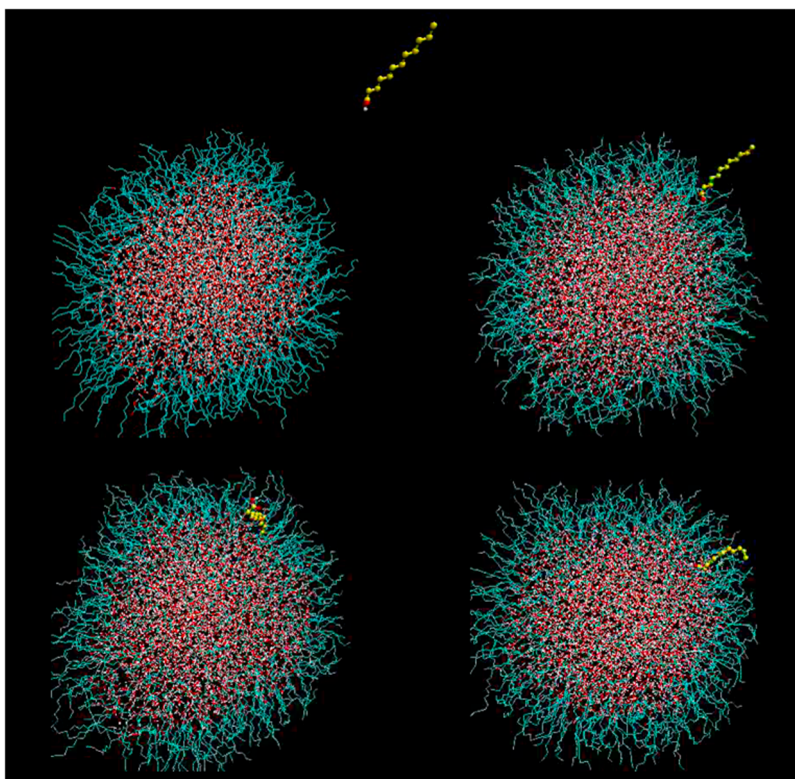


**Figure 2.** Surfactant molecule impinging on the  $^{12}\text{C}$  particle and attaching to the water substrate. Coated particle is  $\sim 8$  nm in diameter and a single surfactant molecule has a length of  $\sim 2$  nm.

snapshot of the equilibrated  $^{28}\text{C}$  particle along with its underlying substrate. In a dramatic departure from the  $^{12}\text{C}/^{20}\text{C}$  particles, the  $^{28}\text{C}$  particle has a highly asymmetric structure where the chains line up “parallel to each other” in some regions forcing significant (local) flattening of the underlying water substrate. This departure from the spherical  $^{5}\text{C}/^{12}\text{C}$  particles is clearer from the radial distribution function (rdf) plot. Figure 4 plots rdFs for the terminal beads of both the  $^{12}\text{C}$  and  $^{28}\text{C}$  particles. The peak for the  $^{12}\text{C}$  particle (where the chains are arranged radially outward) occurs at a distance of around  $4.75 \text{ \AA}$ . If the chains of the  $^{28}\text{C}$  particle were similarly arranged (i.e., radially outward),

one would expect the peak for the  $^{28}\text{C}$  particle to shift further to the right (i.e., the nearest terminal group would be expected to be further away). Using the ball-stick model developed in work by [Chakraborty and Zachariah, 2007], this peak should be expected at approximately  $6.7 \text{ \AA}$ , denoted by the dashed vertical line in Figure 4. However, the peak for the terminal methyl group of the  $^{28}\text{C}$  particle was found at around  $4.25 \text{ \AA}$ , indicating that many of the chains are closer to

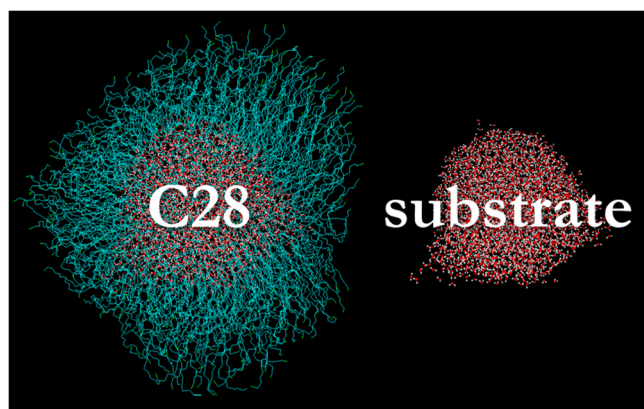


**Figure 3.** Equilibrated  $^{28}\text{C}$  particle along with the underlying substrate. Particle is  $\sim 13$  nm in diameter.

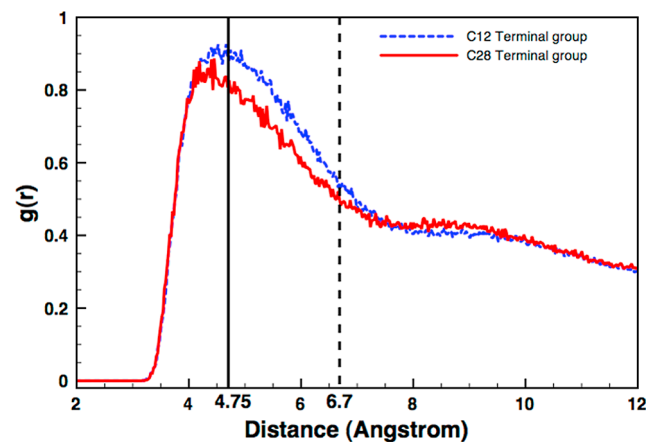


**Figure 4.** Radial distribution functions of the terminal methyl group of  $^{12}\text{C}$  and  $^{28}\text{C}$  particles. The dotted vertical line at  $6.7 \text{ \AA}$  indicates the expected radial distance between terminal methyl groups if the  $^{28}\text{C}$  chains extended out radially.

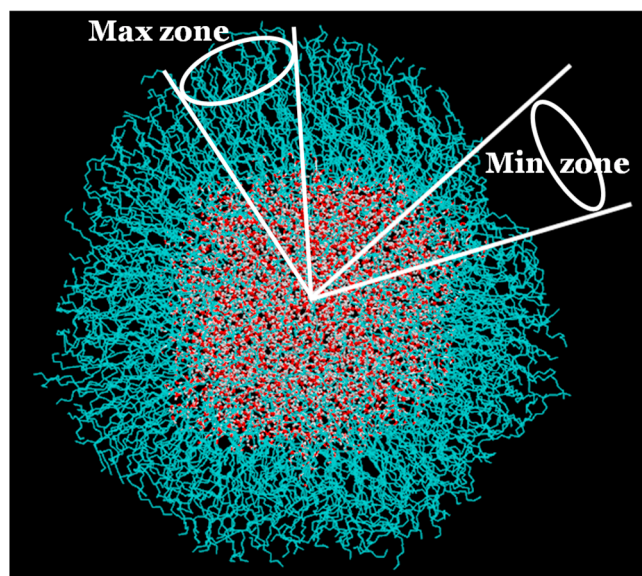


**Figure 5.** Carbon-28 particle with cones marking the minimum and maximum surface coverage zones.

each other for the  $^{28}\text{C}$  particle. This is consistent with the earlier observation that the chains line up parallel to each other and is a result of much stronger chain-chain interaction of the longer chains. As is evident from Figure 3, the underlying water substrate is significantly distorted to accommodate the change in orientation of chains. This water substrate can be divided roughly into two areas: one, relatively flat with high surface coverage (parallel chains) and another, corner-like with much reduced coverage.

[19] As has been widely reported [Blodgett, 1935; Langmuir, 1917], the natural tendency of surfactant molecules on a flat-water substrate is to orient themselves parallel to each other. This is the minimum energy structure. Since, the fatty acid is essentially insoluble in water; small particles consisting of water and insoluble fatty acid have two options. Either, maintain a (minimum energy) spherical water/surfactant interface with the surfactant molecules oriented radially outward, or form a structure with surfactant molecules parallel to each other forcing local flattening of the underlying water substrate. Particles with smaller coatings, e.g.,  $^{5}\text{C}$  and  $^{12}\text{C}$ , prefer the first option. Although the resulting energy in the coating is higher, it is compensated for by the lowered energy of the spherical water/surfactant interface. The interface, deformed from its minimum energy shape, would result in an overall higher energy for the particle. For the  $^{28}\text{C}$  particle, however, there is a significant increase in chain-chain interaction. The increased attraction causes the surfactant molecules to orient themselves parallel to each other, thereby lowering the energy of the coating. Even though the interfacial energy increases in the process, as evidenced by the expanded interface area, the resultant energy of the particle is lower than the corresponding spherical structure.

[20] Sticking coefficient calculations were carried out for the  $^{28}\text{C}$  particle, and *none* of the 100 incident water molecules stuck to this particle.

[21] The particle was then binned into cones to identify the areas of maximum/minimum surfactant coverage (max/min zones). Figure 5 marks the regions of minimum and maximum surface coverages. For both the max and min zones, twenty water molecules were shot toward the particle with the most probable velocity at the particle temperature. As expected, in the zone of maximum coverage density, all the incident water molecules were reflected back (mostly specular reflection, but in a few cases diffuse reflection). This is altogether not surprising since an incoming water molecule would have to effectively break a much stronger (parallel) chain-chain interaction in order to penetrate to the underlying water core. However, the collisions in the min zone, surprisingly, also did not lead to any sticking. Instead of exposing the underlying water substrate, the hydrocarbons in this area lay flat on the water surface. As a result, the incoming water vapor molecules were not able to penetrate the coating. In other words, particles with longer chains would behave as if the surface is *oily* as opposed to the particles with shorter chains, which attract water, thus behaving as if the surface is hydrophilic.

[22] Although this work is focused on the effect of longer/branched chains on the structure and properties of surfactant-coated water droplets, a few words on the effect of substrate curvature are in order. The substrate for each of the particles considered above is a  $\sim 4$  nm (diameter) water droplet. The water-surfactant interface curvature definitely has a big role to play in the final structure of the particle. For example, for a significantly larger substrate, the average distance between adjacent surfactants would be less than that in the present case resulting in increased chain-chain interaction. So, it is reasonable to assume that larger substrates would result in parallel chains along with local flattening of the interface at much shorter chain lengths; thus particles with larger water substrates would be more hydrophobic than those with smaller substrates, for a given chain length.

### 3.3. Phytanic Acid (a Prototype Branched Chain)

[23] Next, to study the effect of fatty acid chain packing, we explore a branched surfactant coating, using phytanic acid. As before, 505 phytanic acid molecules were attached to the surface water molecules. After a short energy minimization step, the particle was allowed to equilibrate. Figure 6 gives a snapshot of the equilibrated particle and its

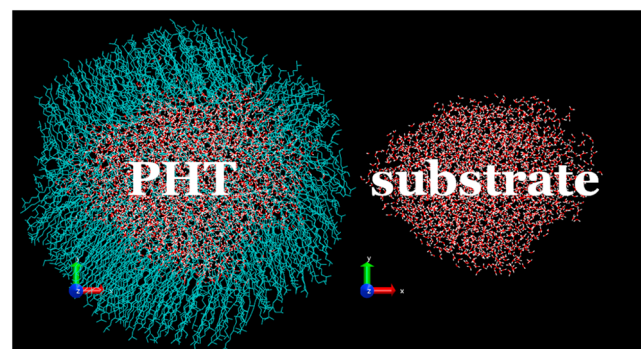


**Figure 6.** Equilibrated water droplet coated with phytanic acid and the underlying water substrate. Particle is  $\sim 8$  nm in diameter.

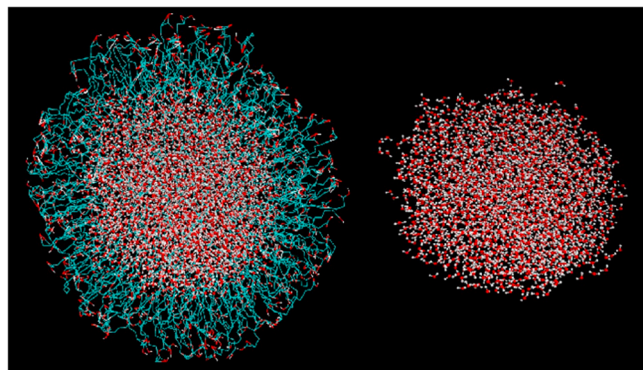


**Figure 7.** Equilibrated  $^{12}\text{C}$  terminal group oxidized particle and the underlying substrate.

water substrate. Although the overall length of a phytanic acid molecule is close to that of a dodecanoic acid ( $^{12}\text{C}$ ) molecule, the branching in the molecules results in a much increased chain-chain interaction. As a result, as in the  $^{28}\text{C}$  particle, significant regions were found where the surfactant molecules line up parallel to each other, forcing the deformation (flattening) of the water-surfactant interface. Thus, it is the overall chain-chain interaction and not just the length of the organic that determines the morphology of the coated structure. As this interaction increases from  $^{12}\text{C}$  to  $^{28}\text{C}$ /PHT, the interface distorts to accommodate the new orientations.

[24] Similar to the case of the  $^{28}\text{C}$  particle, none of the 100 incident water molecules were found to stick to the PHT particle, leading to a zero sticking coefficient. Most of the chains being parallel to each other, there was essentially “no gap” for water vapor to penetrate. The PHT particle, thus, would behave as if the surface is *oily*.

#### 4. A Brief Look at an Acid Terminal Group

[25] *Ellison et al.* [1999] argued that the atmosphere would react with the organic-coated, inverted micelle and transform it. Atmospheric hydroxyl radicals trigger organic free radical reactions leading to the oxidation of marine aerosol particles so that they get coated with, among others,

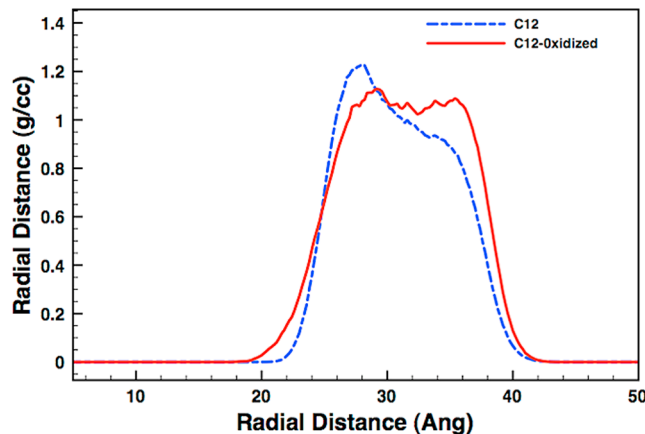


**Figure 8.** Density profiles of the organic coating of the  $^{12}\text{C}$  and  $^{12}\text{C}$ -oxidized particles.

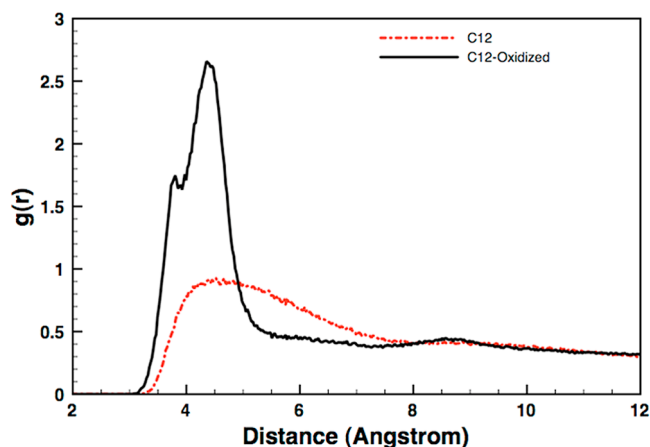


**Figure 9.** Comparison of radial distribution functions (rdfs) for the terminal group of the  $^{12}\text{C}$  and  $^{12}\text{C}$ -oxidized particles.

acid functional groups. It is reasonable to expect that, over time, the hydrocarbon terminal groups would encounter oxidation reactions in the atmosphere. To study the effect of a hydrophilic terminal group on the structure of the particle, and its water-processing capability, the terminal methyl ( $-\text{CH}_3$ ) group of the  $^{12}\text{C}$  particle was replaced with an acid group ( $-\text{COOH}$ ) to form a  $^{12}\text{C}$ -oxidized particle. Figure 7 shows a snapshot of the equilibrated  $^{12}\text{C}$ -oxidized particle, indicating that the oxidized surfactant molecules fold over at the surface (compare Figure 7 with Figure 1). Following equilibration, the density profile of this oxidized particle was computed (Figure 8). The polar terminal group at the surface of the particle folds, resulting in an increase in density at the surface. The increased density effect is most evident in the rdf computation of the carbon atom in the terminal acid group as compared with that of the  $^{12}\text{C}$  particle, shown in Figure 9. Clearly, the terminal group of the oxidized particle has more neighbors, implying that the surfactant molecules do indeed fold over at the surface as argued.

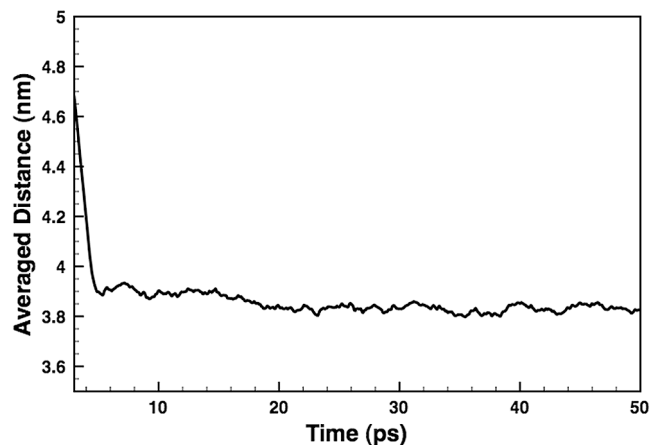


**Figure 10.** Average distance of the incident monomer (averaged over all of the trapped trajectories) from the center of the particle as a function of time.

**Table 2.** Structure Versus Sticking Coefficient

Particle	Structure	Water Vapor Sticking Coefficient
Bare water droplet	Symmetric; spherical water/air interface	1.0
$^5\text{C}$	Symmetric; spherical water/surfactant interface, hydrocarbon chains are oriented "radially outward"	$\sim 0.18$
$^{12}\text{C}$	Same as $^5\text{C}$	$\sim 0.15$
$^{28}\text{C}$	Asymmetric structure; hydrocarbon chains are "parallel to each other" with local flattening of the underlying water substrate	$< 0.01$
PHT	Same as $^{28}\text{C}$	$< 0.01$

[26] The sticking coefficient,  $\alpha$ , was found to be 0.50 for the oxidized particle; that is, one in every two collisions led to a stick. This increase in sticking probability (from one in six/seven collisions for the  $^{12}\text{C}$  particle) can be attributed to the more water-like polar surface of the oxidized particle as opposed to the hydrophobic surface of the  $^{12}\text{C}$  particle. For the trapped cases, the average distance of the monomer (average taken over all the trapped cases) from the center of the particle was computed as a function of time and is plotted in Figure 10. However, the trapped monomers were not seen to penetrate the coating, in contrast to the case for the  $^{12}\text{C}$  particle [Chakraborty and Zachariah, 2008]. Instead they stick to the largely polar surface as there is, again, no gap between the oxidized fatty acid molecules (lower permeability) for the monomers to diffuse through. Also, the diffusion rate of water through a dense network of polymers being very small, it would take long times, of the order of hundreds of nanoseconds (beyond the scope of our current computational capabilities), for water to penetrate the coating. The important point here is that in the context of the prior observation that the water droplets coated with amphiphilic chains (with negative surface tension) are water processors, which enable the water to penetrate to the core (underlying water droplet), these structures would simply have the usual vapor pressure relationships, which may mimic the more traditional two component mixed organic-water systems usually addressed by a Kohler analysis, more typically found for a water droplet.

[27] The  $^{28}\text{C}$  particle, on the other hand, is not expected to have a significantly different structure following oxidation of its terminal group. The  $^{28}\text{C}$ -oxidized chains, being considerably longer, would have the terminal group further away from the water substrate than their  $^{12}\text{C}$ -oxidized counterparts and would not "fold over" to be closer to the polar water surface.

## 5. Summary

[28] The main results are summarized in Table 2. The particles coated with shorter-chain fatty acids ( $^5\text{C}$  and  $^{12}\text{C}$ ) would have a pressure profile going negative in the region of the organic coating resulting in a negative surface tension. This negative surface tension in turn would lead to an inverse Kelvin vapor pressure effect (increased condensation). It may then be argued that, if the interface energy dominates, the structure of the inverse micelle will be spherical leading to a negative surface pressure and tension, and result in significant enhancement in water-processing

capability. On the other hand, if the chains are long enough (or are branched) such that chain-chain interactions are significantly greater, then they will tend to align as much as possible parallel to each other, and result in deformation of the underlying water droplet. A zero value in the rate of water uptake shows that these particles will act very much like an *oily* surface. Hence, depending on the length and branching of the organics coating the particle, we would either have a net water attractor or an oily droplet.

## References

- Allen, M. P., and D. J. Tildesley (1987), *Computer Simulation of Liquids*, Oxford Univ. Press, New York.
- Baier, R. E. (1972), Organic films on natural waters: Their retrieval, identification, and modes of elimination, *J. Geophys. Res.*, 77(27), 5062–5075, doi:10.1029/JC077i027p05062.
- Berendsen, H. J. C., J. P. M. Postma, W. F. van Gunsteren, and J. Hermans (1981), Interaction models for water in relation to protein hydration, in *Intermolecular Forces*, edited by B. Pullman, pp. 331–342, Reidel, Dordrecht, Netherlands.
- Berendsen, H. J. C., J. R. Grigera, and T. P. Straatsma (1987), The missing term in effective pair potentials, *J. Phys. Chem.*, 91(24), 6269–6271, doi:10.1021/j100308a038.
- Berendsen, H. J. C., D. van der Spoel, and R. van Drunen (1995), GROMACS: A message-passing parallel molecular dynamics implementation, *Comput. Phys. Commun.*, 91(1–3), 43–56, doi:10.1016/0010-4655(95)00042-E.
- Blanchard, D. C. (1964), Sea-to-air transport of surface active material, *Science*, 146(3642), 396–397, doi:10.1126/science.146.3642.396.
- Blodgett, K. B. (1935), Films built by depositing successive monomolecular layers on a solid surface, *J. Am. Chem. Soc.*, 57(6), 1007–1022, doi:10.1021/ja01309a011.
- Chakraborty, P., and M. R. Zachariah (2007), "Effective" negative surface tension: A property of coated nanoaerosols relevant to the atmosphere, *J. Phys. Chem. A*, 111(25), 5459–5464, doi:10.1021/jp070226p.
- Chakraborty, P., and M. R. Zachariah (2008), Sticking coefficient and processing of water vapor on organic-coated nanoaerosols, *J. Phys. Chem. A*, 112(5), 966–972, doi:10.1021/jp076442f.
- Clifford, D., T. Bartels-Rausch, and D. Donaldson (2007), Suppression of aqueous surface hydrolysis by monolayers of short chain organic amphiphiles, *Phys. Chem. Chem. Phys.*, 9(11), 1362–1369, doi:10.1039/B617079J.
- Ellison, G. B., A. F. Tuck, and V. Vaida (1999), Atmospheric processing of organic aerosols, *J. Geophys. Res.*, 104(D9), 11,633–11,641, doi:10.1029/1999JD900073.
- Gill, P. S., T. E. Graedel, and C. J. Weschler (1983), Organic films on atmospheric aerosol particles, fog droplets, cloud droplets, raindrops, and snowflakes, *Rev. Geophys.*, 21(4), 903–920, doi:10.1029/RG021i004p00903.
- Gilman, J., and V. Vaida (2006), Permeability of acetic acid through organic films at the air-aqueous interface, *J. Phys. Chem. A*, 110(24), 7581–7587, doi:10.1021/jp061220n.
- Husar, R. B., and W. R. Shu (1975), Thermal analyses of Los Angeles smog aerosol, *J. Appl. Meteorol.*, 14(8), 1558–1565, doi:10.1175/1520-0450(1975)014<1558:TAOTLA>2.0.CO;2.
- Langmuir, I. (1917), The constitution and fundamental properties of solids and liquids. II. liquids, *J. Am. Chem. Soc.*, 39(9), 1848–1906, doi:10.1021/ja02254a006.

- Li, J. S., and G. Wilemski (2006), A structural phase diagram for model aqueous organic nanodroplets, *Phys. Chem. Chem. Phys.*, *8*(11), 1266–1270, doi:10.1039/b518305g.
- Lindahl, E., B. Hess, and D. van der Spoel (2001), GROMACS 3.0: A package for molecular simulation and trajectory analysis, *J. Mol. Model.*, *7*(8), 306–317, doi:10.1007/s008940100045.
- Lopez, C. F., P. B. Moore, J. C. Shelley, M. Y. Shelley, and M. L. Klein (2002), Computer simulation studies of biomembranes using a coarse grain model, *Comput. Phys. Commun.*, *147*(1–2), 1–6, doi:10.1016/S0010-4655(02)00195-9.
- Ma, X., P. Chakraborty, B. Henz, and M. Zachariah (2011), Molecular dynamic simulation of dicarboxylic acid coated aqueous aerosol: Structure and processing of water vapor, *Phys. Chem. Chem. Phys.*, *13*, 9374–9384, doi:10.1039/c0cp01923b.
- MacIntyre, F. (1972), Flow patterns in breaking bubbles, *J. Geophys. Res.*, *77*(27), 5211–5228, doi:10.1029/JC077i027p05211.
- MacIntyre, F. (1974), The top millimeter of the ocean, *Sci. Am.*, *230*(5), 62–77, doi:10.1038/scientificamerican0574-62.
- Middlebrook, A. M., D. M. Murphy, and D. S. Thomson (1998), Observations of organic material in individual marine particles at Cape Grim during the First Aerosol Characterization Experiment (ACE 1), *J. Geophys. Res.*, *103*(D13), 16,475–16,483, doi:10.1029/97JD03719.
- Park, S., D. Burden, and G. Nathanson (2007), The inhibition of N<sub>2</sub>O<sub>5</sub> hydrolysis in sulfuric acid by 1-butanol and 1-hexanol surfactant coatings, *J. Phys. Chem. A*, *111*(15), 2921–2929, doi:10.1021/jp068228h.
- Plimpton, S. (1995), Fast parallel algorithms for short-range molecular dynamics, *J. Comput. Phys.*, *117*(1), 1–19, doi:10.1006/jcph.1995.1039.
- Ryckaert, J. P., G. Ciccotti, and H. J. C. Berendsen (1977), Numerical integration of the Cartesian equations of motion of a system with constraints: Molecular dynamics of *n*-alkanes, *J. Comput. Phys.*, *23*(3), 327–341, doi:10.1016/0021-9991(77)90098-5.
- Shelley, J. C., M. Y. Shelley, R. C. Reeder, S. Bandyopadhyay, and M. L. Klein (2001a), A coarse grain model for phospholipid simulations, *J. Phys. Chem. B*, *105*(19), 4464–4470, doi:10.1021/jp010238p.
- Shelley, J. C., M. Y. Shelley, R. C. Reeder, S. Bandyopadhyay, P. B. Moore, and M. L. Klein (2001b), Simulations of phospholipids using a coarse grain model, *J. Phys. Chem. B*, *105*(40), 9785–9792, doi:10.1021/jp011637n.
- Tervahattu, H., J. Juhanoja, and K. Kupiainen (2002), Identification of an organic coating on marine aerosol particles by TOF-SIMS, *J. Geophys. Res.*, *107*(D16), 4319, doi:10.1029/2001JD001403.
- Tervahattu, H., J. Juhanoja, V. Vaida, A. F. Tuck, J. V. Niemi, K. Kupiainen, M. Kulmala, and H. Vehkamäki (2005), Fatty acids on continental sulfate aerosol particles, *J. Geophys. Res.*, *110*, D06207, doi:10.1029/2004JD005400.
- Thornton, J., and J. Abbatt (2005), N<sub>2</sub>O<sub>5</sub> reaction on submicron sea salt aerosol: Kinetics, products, and the effect of surface active organics, *J. Phys. Chem. A*, *109*(44), 10,004–10,012, doi:10.1021/jp054183t.
- Vieceli, J., M. Roeselova, and D. J. Tobias (2004), Accommodation coefficients for water vapor at the air/water interface, *Chem. Phys. Lett.*, *393*(1–3), 249–255, doi:10.1016/j.cplett.2004.06.038.
- Wyslouzil, B. E., G. Wilemski, R. Strey, C. H. Heath, and U. Dierregswiler (2006), Experimental evidence for internal structure in aqueous-organic nanodroplets, *Phys. Chem. Chem. Phys.*, *8*(1), 54–57, doi:10.1039/b514824c.

---

P. Chakraborty and M. R. Zachariah, University of Maryland, College Park, MD 20742, USA. (mrz@umd.edu)